

## Modulation of human P-glycoprotein epitope expression by temperature and/or resistance-modulating agents

Bénédicte Jachez,<sup>1</sup> Maurizio Cianfriglia<sup>2</sup> and Francis Loor<sup>1,3</sup>

<sup>1</sup>Preclinical Research, Sandoz Pharma Ltd, 386/643, CH 4002 Basel, Switzerland. Tel: (+41) 61 324 5365; Fax: (+41) 61 324 4787. <sup>2</sup>Laboratorio di Immunologia, Istituto Superiore di Sanita, Viale Regina 299, I 00161 Roma, Italy. <sup>3</sup>Immunology Laboratory, Strasbourg 1 University, BP 24, F 67401 Illkirch, France.

Three monoclonal antibodies (mAb), MRK16, MM4.17 and MC57, directed against distinct epitopes on the external domain of human P-glycoprotein (Pgp), were used to follow its expression on multidrug resistant (MDR)-cells. The linear MM4.17 epitope and conformational MRK16 epitope showed a 4-fold higher expression at 37°C than at 4°C, while the detection of the conformational MC57 epitope did not change. Inhibition of Pgp function, by a short pretreatment of the MDR-cells with resistance-modulating agents (RMA), such as SDZ PSC 833 and SDZ 280-446, could not be related to depletion of Pgp from the cell surface, since their expression of the MM4.17 and MRK16 epitopes was found unchanged. However, a substantially higher expression of MC57 epitopes was found on RMA-treated cells than on untreated ones. Since this effect correlated to the strength of different RMA in reversing the MDR phenotype, MC57 epitopes might be more efficiently expressed on inactivate(d) forms of the Pgp molecules, suggesting that RMA might inhibit Pgp function by disturbing the conformation of individual Pgp molecules, their topographical distribution or polymerization status in the membrane.

**Key words:** Epitope expression, chemosensitizer, multidrug resistance, P-glycoprotein, SDZ PSC 833.

### Introduction

A major mechanism by which tumor cells become resistant to anti-cancer drugs (ACD) is by decreasing intracellular ACD bioavailability. Such a multidrug resistance (MDR) phenotype of the tumor cells is usually mediated by the overexpression of *mdr-1* gene-encoded P-glycoprotein (Pgp) molecules which pump drugs out of the cells by an ATP-dependent process.<sup>1-3</sup>

---

The Laboratoire d'Immunologie at the Strasbourg 1 University was supported by grants from the Association de Recherches sur le Cancer (Villejuif, France), the Ligue du Haut-Rhin contre le Cancer (Colmar, France) and Sandoz Pharma Ltd (Basel, Switzerland).

---

Correspondence to F Loor

A major pharmacological approach consists of trying to inhibit the Pgp pump function enough to restore sensitivity to the classical ACD within the range of dosages compatible with their *in vivo* therapeutic window.<sup>2</sup> A variety of resistance modulating agents (RMA) now available could either inhibit MDR and/or interfere with the ACD binding to Pgp, the earliest identified RMA being quinidine and verapamil. The structures of such RMA are as widely different as the structures of the ACD which are Pgp substrates.<sup>2</sup>

In this paper, three different monoclonal antibodies (mAb) directed against distinct external domains of the human *mdr-1* gene-encoded Pgp, MC57, MM4.17 and MRK16, were used to study Pgp expression on RMA-treated MDR-cells. All three anti-Pgp mAb belonged to the IgG2a isotype and could be used for detection of Pgp on intact cells by immunofluorescence. The MC57 epitope, i.e. the Pgp epitope recognized by MC57, is a conformational Pgp epitope<sup>4</sup> (Cianfriglia *et al.*, in preparation). The MM4.17 epitope is a continuous epitope made of eight amino acids on the fourth external loop of Pgp.<sup>5</sup> The MRK16 epitope is a discontinuous epitope involving sequences from the first and fourth external loop of the Pgp, separated by about 625 amino acids in the linear sequence.<sup>6</sup>

Our previous data<sup>7</sup> suggested that some RMA, at least the cyclosporin derivative SDZ PSC 833<sup>8,9</sup> and the novel semi-synthetic cyclopeptolide SDZ 280-446,<sup>9,10</sup> might induce a long-lasting depletion of functional Pgp from the MDR-cell surface. This RMA-induced 'knock out' of the Pgp function could be interpreted in various ways, such as a sorting out of the Pgp from the MDR-cell membrane, an irreversible binding to the Pgp, major alterations in the distribution of Pgp molecules in the membrane with their inactivation by either the clustering of functional Pgp monomers or the dispersion of functional Pgp polymers. Facing such a variety of possible explanations, it was mandatory to determine the

fate of membranous Pgp after treatment with the RMA. This was analyzed here, on untreated and RMA-treated cells, by using three human MDR-cell lines (CEM, KB and LoVo) and three different mAb directed to extracellular Pgp epitopes.

## Materials and methods

### mAb

The three different anti-Pgp mAb used in these studies were of BALB/c origin and IgG2a isotype. They recognized different epitopes of the human *mdr-1* encoded Pgp exposed on the external surface of intact tumor cells. Two of them were developed by one of us (MC) at the Istituto Superiore di Sanita, Roma, Italy. The MM4.17 source was a culture supernatant of hybridoma and the MC57 source was an ascitic fluid. The third anti-Pgp mAb was MRK16, which was purchased from Kamiya Biomedical Company (Thousand Oaks, CA).

### Human tumor cell lines

We used human cell lines which belong to three different cell classes: the adherent nasopharyngeal carcinoma KB.3.1 (Par-KB) and its MDR variant KB-V.1 (MDR-KB, obtained through vinblastine-resistance selection),<sup>11</sup> the adherent colon epithelial carcinoma LoVo/N (Par-LoVo) and its MDR variant LoVo/Dx (MDR-LoVo, obtained through doxorubicin-resistance selection),<sup>12</sup> and the non adherent T-cell leukemia CEM-CCRF.Ø (Par-CEM) and its MDR variant CEM-CCRF.ActD (MDR-CEM, obtained through actinomycin D-resistance selection).<sup>13,14</sup> The MDR variants were continuously grown in the presence of the drug used for their selection (for more details on culture media, see refs 8 and 15). Two pairs of adherent cell lines (KB and LoVo), used for preliminary experiments only, were cultured on glass coverslips for staining and microscopic observation. For convenience, all quantitative and qualitative FACScan analyses were made with the pair of non-adherent T cell leukemia CEM lines.

### General immunostaining procedure for flow cytometry and fluorescence microscopy

Coverslip-grown adherent cells were directly stained for microscopic observation, whereas

non-adherent cells were dispensed in 96-well microtiter plates ( $5 \times 10^5$  cells/well). They were incubated for 30 min on melting ice with 50 µl of anti-Pgp mAb at the adequate dilution in ice-cold PBS containing 1% BSA and 10 mM NaN<sub>3</sub> (PBS/BSA/NaN<sub>3</sub>). After four washes with cold PBS/BSA/NaN<sub>3</sub>, the cell membrane-bound anti-Pgp mAb were detected by exposing the cells for 7 min (on melting ice) to 50 µl of an adequate dilution in PBS/BSA/NaN<sub>3</sub> of a directly FITC-labeled F(ab')<sub>2</sub> rat antibody directed against mouse IgG (RMIGG.FITC; Southern Biotechnology Associates Inc, Birmingham, AL). After further washes with PBS/BSA/NaN<sub>3</sub>, the cells were fixed for 20 min at room temperature with 3.7% formaldehyde in PBS. The cell fluorescence pattern was analyzed by microscopic observation (Ortholux II; Leitz Leica Microscopie und System GmbH, Wetzlar, Germany) and/or the fluorescence levels of individual cells were determined with a FACScan (Becton Dickinson, Mountain View, CA) in order to get a fluorescence profile of the whole cell population.

### Special studies of the effects of various RMA treatment procedures

The presence or absence of RMA during three major phases of the assay: 'pre-incubation/binding of anti-Pgp mAb/detection with fluorescent antibody' allowed the definition of four different procedures.

(+/-/-) or 'pretreatment' procedure. The cells were first incubated (for 30 min at 37°C in the CO<sub>2</sub> incubator) in the presence of the RMA. Following this pre-treatment, the cells were washed with PBS/BSA/NaN<sub>3</sub> and further processed as for the general immunostaining procedure. Thus, the RMA was not present when the cells were antibody-treated.

(+ /+ /+) or 'continuous treatment' procedure. The cells were pretreated with the RMA as above, but the RMA remained present throughout the further procedure, i.e. it was present at the selected concentration in all media, including those used for washing the cells, and for all the staining steps.

(- /+ /+) or 'co-treatment' procedure. The cells were exposed simultaneously to the RMA and the anti-Pgp mAb, without any RMA pretreatment. The exposure to the RMA continued until cell fixation, i.e. during all further washing and staining steps.

(-/-/+) or 'posttreatment' procedure. The RMA was added only after anti-Pgp mAb binding and mAb excess washing. Then, the RMA was kept until cell fixation. Thus, the RMA was present in the medium only during the detection of the membrane-bound anti-Pgp mAb by the fluorescent anti-mouse Ig antibody.

#### General procedure for the measurement of daunomycin (DAU) retention

The protocol was adapted for microplates from previous studies.<sup>16</sup> Briefly, the DAU loading step was performed by incubating  $5 \times 10^5$  cells for 30 min at 37°C in a humidified atmosphere enriched with 7% CO<sub>2</sub> in the presence of 20 µM DAU (Sigma D-4885 St Louis, MO) and of various concentrations of RMA or its solvent. After washes, the DAU efflux step was performed by reincubating the cells for 15 min at 37°C in culture medium only. The measurement of the DAU retained in the cells was performed by washing and fixing the cells with PBS containing 3.7% formaldehyde and measuring their DAU-specific fluorescence with a FACScan (Becton Dickinson) equipped with an argon laser (15 mW) tuned at 488 nm. Dead cells and debris were excluded by setting a gate on the basis of their decreased forward light scatter.

#### Presentation of the data from FACScan analyses

In the fluorescence histograms, the *x*-axis was a logarithmic scale for the fluorescence level and the *y*-axis was an arithmetic scale for the number of cells recorded in each channel. In order to facilitate comparisons, some histograms were then overlayed on a single diagram.

In order to simplify the comparison of a large number of cell fluorescence profiles, the *levels* of DAU retention or of Pgp-specific fluorescence staining were most often expressed as percentages of the fluorescence of adequate controls. Thus, for the effects of RMA treatment on DAU retention, DAU retention in MDR cells was expressed as a percentage of the retention obtained with similarly treated Par cells: [(mean fluorescence of RMA-treated MDR-cells/mean fluorescence of RMA-treated Par-cells) × 100].

In cases where the specific anti-Pgp mAb fluorescence was measured, the effects of RMA treatment on mAb staining were expressed as [(mean fluorescence of RMA-treated, mAb-stained cells/mean

fluorescence of solvent-treated, mAb-stained cells) × 100]; the effect of temperature on anti-Pgp mAb staining was measured as (mean fluorescence of mAb-stained cells processed at 37°C/mean fluorescence of mAb-stained cells processed at 0°C). Other comparisons were done on similar principles (see Results).

Since the shape of the fluorescence profiles of given cell populations could vary from a broad to narrow type distribution, depending on the staining conditions or on the anti-Pgp mAb used, we arbitrarily defined an 'index of population homogeneity', which was defined by the ratio of the height of the fluorescence profile by its width measured at the half of its height. Thus, the highest values corresponded to the more homogeneous cell fluorescence profiles of the MDR-cell population.

#### Statistical analyses

The significance of the reversion of the DAU retention induced by the RMA was evaluated by using the Wilcoxon signed rank sum test for paired data.

The effects of RMA or temperature on the intensity or the homogeneity of the cell population staining were expressed as ratios of the values obtained for RMA-treated cells by the ones of solvent-treated cells. The significance of these effects were evaluated by comparing the mean values of the ratios to the theoretical values of 1 (or 100%) obtained in absence of effect, by using the table of *t*-distributions.

#### Results

##### Enhanced MC57-mediated Pgp detection on SDZ PSC 833-pretreated MDR-LoVo, MDR-KB and MDR-CEM cells

The MDR-cells were briefly exposed to the RMA which was washed away before the staining of the cells with the anti-Pgp mAb. Indeed, our goal was to find out whether the RMA had induced a disappearance of the Pgp molecules from the cell surface. This 'pretreatment' protocol is referred as '+/-/-' (see Materials and methods).

This was done first with adherent MDR-cells grown and stained on glass coverslips. Surprisingly, MDR-cells which had been pretreated with SDZ PSC 833 at 10 or 100 µg/ml (MDR-KB cells) or 50 µg/ml (MDR-LoVo cells) displayed a brighter MC57 epitope-specific membrane fluorescence

than their controls (ethanol-pretreated MDR-cells). However, the evaluation of the Pgp expression level was limited to the visual estimation.

In order to quantitate this effect of SDZ PSC 833, further experiments were done with a third, non-adherent, human cell line, the MDR-CEM cell line. Its pretreatment with SDZ PSC 833 also enhanced MC57 binding. Furthermore, the enhancement seemed to be dependent on the SDZ PSC 833 concentration. Indeed, when the fluorescence of the SDZ PSC 833-treated cells was expressed as a percentage of the fluorescence of the ethanol-treated cells, we obtained the following results: 96, 157 and 379% for, respectively, 0.1, 1.0 and 10  $\mu\text{g}/\text{ml}$  of SDZ PSC 833. Nevertheless, the Pgp detection enhancement might have been a peculiarity of SDZ PSC 833.

#### Enhanced MC57 epitope detection on MDR-CEM cells exposed to various RMA

In order to know whether other RMA might also induce such an enhancement of Pgp detection, SDZ 280-446, SDZ PSC 833 and cyclosporin A (CsA) [all at 10  $\mu\text{g}/\text{ml}$  (about 8  $\mu\text{M}$ )] and verapamil (at 10  $\mu\text{M}$ ) were assayed for their capacity to alter MC57 binding. Both cyclosporins and the cyclopeptolide could shift the cell population profile to higher fluorescence. CsA, which is a weaker RMA than SDZ PSC 833 and SDZ 280-446, caused a smaller fluorescence shift, whereas the weakest RMA, verapamil, did not cause any shift (Figure 1). To investigate whether this enhancement of the Pgp detection was indeed related to the RMA efficacy in reversing the MDR phenotype, the capacity of the cells to efflux DAU was further studied. Thus, following pretreatment with those RMA or their solvent (ethanol), the cells were either stained with MC57 or processed through the DAU retention assay (Table 1). Three out of the four RMA tested (SDZ PSC 833, SDZ 280-446 and CsA, but not verapamil) were able to enhance both the DAU retention in MDR-CEM cells and the Pgp detection on MDR-CEM cells. The same ordering was obtained when RMA were classified according to their capacity to restore the DAU retention or their ability to enhance the Pgp staining.

#### Enhancement of MC57 epitope detection

To further study how the RMA might induce a higher expression of Pgp molecules, the cells were ex-

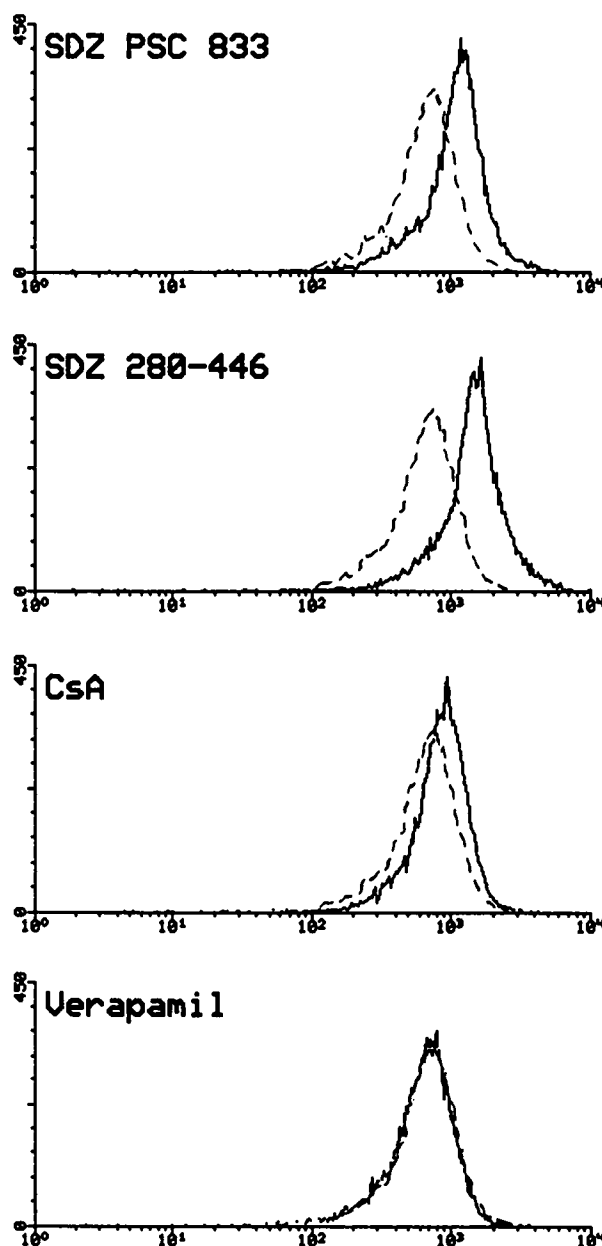


**Figure 1.** Effect of four different RMA on the Pgp detection by the MC57 in one representative experiment. The fluorescence intensities (x-axes, logarithmic scale) are shown as a function of the MDR-cell numbers in each channel (y-axes, linear scale). MDR-CEM cells were pretreated, 30 min before the Pgp staining, with either the RMA (plain lines, at 10  $\mu\text{g}/\text{ml}$  for SDZ PSC 833, SDZ 280-446 and CsA, and 10  $\mu\text{M}$  for verapamil), or its solvent alone (dotted lines). SDZ PSC 833, SDZ 280-446 and CsA but not verapamil were able to enhance the Pgp detection by MC57.

posed to RMA at various steps during the Pgp detection. Besides the pretreatment (+/-/-) procedure in which the cells were exposed to the RMA only prior to the Pgp detection, three different

**Table 1.** RMA activity on DAU retention and Pgp detection using CEM couple of cell lines.

RMA ( $\mu\text{g/ml}$ or $\mu\text{M}$ ) <sup>a</sup>		DAU retention <sup>b</sup>	MC57-mediated Pgp detection <sup>c</sup>
Ethanol		1.8 $\pm$ 0.5	100
SDZ PSC 833	(1)	3.5 $\pm$ 1.0 <sup>d</sup>	169 $\pm$ 19 <sup>e</sup>
	(10)	9.8 $\pm$ 2.7 <sup>d</sup>	192 $\pm$ 33 <sup>f</sup>
SDZ 280-446	(1)	4.4 $\pm$ 0.9 <sup>d</sup>	235 $\pm$ 50 <sup>d</sup>
	(10)	9.2 $\pm$ 4.0 <sup>d</sup>	242 $\pm$ 54 <sup>f</sup>
CsA	(1)	1.9 $\pm$ 0.6	103 $\pm$ 7
	(10)	3.3 $\pm$ 0.8 <sup>d</sup>	149 $\pm$ 21 <sup>f</sup>
Verapamil	(1)	1.8 $\pm$ 0.5	98 $\pm$ 3
	(10)	2.5 $\pm$ 0.7 <sup>d</sup>	107 $\pm$ 12

<sup>a</sup>The actual concentrations used were 1 and 10  $\mu\text{M}$  for verapamil, and 1 and 10  $\mu\text{g/ml}$  (about 0.8 and 8  $\mu\text{M}$ ) with SDZ PSC 833, SDZ 280-446 and CsA.

<sup>b</sup>DAU retention in MDR-CEM cells was expressed as percentage of the retention obtained in similarly treated Par-CEM cells. Results were the mean values  $\pm$  SD of nine to 10 independent experiments.

<sup>c</sup>MC57 binding to the MDR-CEM cells was calculated as follows: (mean fluorescence of the RMA-treated cells/mean fluorescence of ethanol-treated cells)  $\times$  100. Results were the mean values  $\pm$  SD of four and seven independent experiments performed with, respectively, 1 and 10  $\mu\text{M}$  (or  $\mu\text{g/ml}$ ) RMA.

<sup>d</sup> $p < 0.01$ , in comparison with ethanol control, by the Wilcoxon signed rank test (paired observations).

<sup>e</sup> $p < 0.02$  in comparison of the mean to the value of 100, expected in absence of RMA effect, by using the table of  $t$  distributions.

<sup>f</sup> $p < 0.001$ , in comparison of the mean to the value of 100, expected in absence of RMA effect, by using the table of  $t$  distributions.

procedures were then assayed. In the continuous treatment (+/+ /+) procedure, the RMA were present both before and throughout the whole Pgp detection procedure. In the co-treatment (-/+ /+) procedure, the RMA were present only during the whole Pgp detection procedure but not before; in this case, the RMA could not alter the Pgp expression, prior to the binding of MC57, but they could interfere with the binding and redistribution of both MC57 and its revealing antibodies. Finally, in the posttreatment (-/- /+) procedure, the RMA were added only during the exposure of the cells to the fluorescent anti-mouse Ig antibody; in the latter case, the RMA should not alter the expression of Pgp nor its detection by MC57, although they might still alter the detectability of the complexes by the fluorescent antibodies. The RMA were used at 10  $\mu\text{g/ml}$  (about 8  $\mu\text{M}$ ) for the cyclic peptides and 10  $\mu\text{M}$  for verapamil. Their effects on the Pgp detection in the different procedures are shown in Table 2.

The clearest fact was that, in posttreatment (-/- /+) conditions, i.e. when the RMA were added after binding of MC57 to the membrane-expressed Pgp, none of the tested RMA changed the level of the Pgp detection. The comparison of the co-treatment (-/+ /+) with the continuous treatment (+/+ /+) procedures showed that a pre-exposure of the MDR-CEM cells to the RMA was not a prerequisite to see the

enhanced detectability of Pgp.

For SDZ PSC 833, SDZ 280-446 and CsA, even the pretreatment (+/- /-) was sufficient to increase Pgp detection substantially and the continuous treatment (+/+ /+) or cotreatment only (-/+ /+) did not bring about a further increase of Pgp detection. Rather, there might be a slight decrease, but the continuous presence (+/+ /+) of the cyclic peptides during exposure of the cells to the antibodies (MC57 and fluorescent anti-mouse Ig) definitely did not inhibit antibody binding. In the case of verapamil, the comparison of the data from all four treatment conditions suggested that, in order to favor Pgp detection, verapamil had to be present on the cells during their exposure to MC57 (Table 2).

To further characterize the kinetics of that striking enhancement of the Pgp detection, the exposure to the RMA in pretreatment (+/- /-) conditions was varied from 5 to 30 min. The RMA-mediated effect on the Pgp detection was a fast event, as a 5 min pretreatment led to the same effect as a 30 min one. Moreover, the membrane dynamics did not seem to play a major role in this event. Performing the RMA pretreatments at 37 or at 0°C (on ice) gave similar effects. Finally, addition of a capping inhibitor ( $\text{NaN}_3$  at 10 mM) did not change the RMA-mediated enhancement of the Pgp detection (data not shown).

**Table 2.** Effect of various RMA treatment procedures on the Pgp detection by MC57<sup>a</sup>

RMA <sup>c</sup>	Procedure (N) <sup>b</sup>			
	+/-/- (5)	+/+ (4)	-/+ (4)	-/-/+ (3)
Ethanol	100	100	100	100
SDZ PSC 833	181 ± 32 <sup>d</sup>	168 ± 27 <sup>d</sup>	145 ± 5 <sup>e</sup>	99 ± 2
SDZ 280-446	228 ± 33 <sup>e</sup>	213 ± 41 <sup>d</sup>	205 ± 34 <sup>d</sup>	97 ± 2
CsA	139 ± 8 <sup>e</sup>	117 ± 6 <sup>d</sup>	142 ± 16 <sup>d</sup>	103 ± 4
Verapamil	112 ± 10	135 ± 7 <sup>d</sup>	145 ± 6 <sup>e</sup>	103 ± 3

<sup>a</sup>The data report the mean values (± SD) of the cell fluorescence, calculated as follows: (mean fluorescence of RMA-treated cells/mean fluorescence of ethanol-treated cells) × 100; for details on the different procedures, see text.

<sup>b</sup>(N) = number of independent experiments performed by each procedure.

<sup>c</sup>10 µg/ml (about 8 µM) for SDZ PSC 833, SDZ 280-446 and CsA, 10 µM for verapamil.

<sup>d</sup>*p* < 0.02, in comparison of the mean to the value of 100, expected in absence of RMA effect, by using the table of *t* distributions.

<sup>e</sup>*p* < 0.001, in comparison of the mean to the value of 100, expected in absence of RMA effect, by using the table of *t* distributions.

#### Comparison of MC57 with two other anti-Pgp mAb (MM4.17 and MRK16) for Pgp detection on MDR-CEM cells not exposed to a RMA

When MDR-cells were not exposed to any RMA and directly stained on ice (general immunostaining conditions), all three anti-Pgp mAb gave similar fluorescence profiles in flow cytometry. However, some differences were revealed when the Pgp staining was performed at 37°C. The binding of MM4.17 and MRK16 to the Pgp-expressing cells was about four times higher at 37°C than on ice, whereas the binding of MC57 was unaffected by the temperature shift. The ratios between fluorescence indices obtained at 37 and 0°C (mean values ± SD, *p* values if significant) obtained in four to six independent experiments were 4.09 ± 0.6 for MM4.17 (*p* < 0.01), 3.89 ± 1.13 for MRK16 (*p* < 0.01) and 1.18 ± 0.6 for MC57. A representative experiment is shown in Figure 2.

Various redistribution phenomena, which could occur at 37°C (normal membrane fluidity) but not at 0°C (reduced membrane fluidity), might have stabilized the interactions of Pgp molecules with some anti-Pgp mAb and be responsible for the enhanced binding. The distribution of the membranous fluorescence was thus compared by fluorescence microscopy on cells which had interacted with anti-Pgp mAb at 0 or 37°C, but no altered patterns, such as patching or capping, were found.

In the case of MM4.17-mediated Pgp staining, the temperature influenced not only the staining intensity but also its homogeneity. In fact, the population profiles of MM4.17-stained cells were more homogeneous at 37°C: within each individual experiment,

the flow cytometry profiles were narrower and higher for cells stained at 37°C than for cells stained at 0°C (Figure 2). This lower dispersion of cell fluorescence levels was quantitated as an homogeneity index (as defined in the Material and methods section) and it varied from one experiment to the other [individual values can be seen as ethanol controls for the RMA-treated samples shown in a later section (Figure 5)]. Nevertheless, data obtained from four to seven independent experiments showed that, in comparison with the homogeneity indices of cells stained with MM4.17 at 0°C (2.2 ± 0.5), those of cells stained at 37°C (3.2 ± 0.9) were higher (135 ± 23%, *p* < 0.05), whereas similar calculations did not show significant differences for staining with MC57 (115 ± 20%) or MRK16 (99 ± 35%). Thus, it was a specific feature of MM4.17 epitope recognition.

#### Effects of RMA on the detection of MC57, MM4.17 and MRK16 epitopes

Enhancement of the Pgp detection by RMA-pretreated cells might be restricted to MC57 epitopes. Therefore, the two other anti-Pgp mAb (MM4.17 and MRK16) were used to detect Pgp on RMA-pretreated cells. Only SDZ PSC 833 and SDZ 280-446 were used as they had the strongest effect on the Pgp detection by MC57.

In fact, the effect of RMA-pretreatment on Pgp detection could depend on the anti-Pgp mAb used and on the staining temperature (Figure 3). MC57 binding to Pgp was enhanced by pretreatment with each RMA (*p* < 0.01 for SDZ PSC 833 and *p* < 0.001 for SDZ 280-446) whatever the staining tempera-

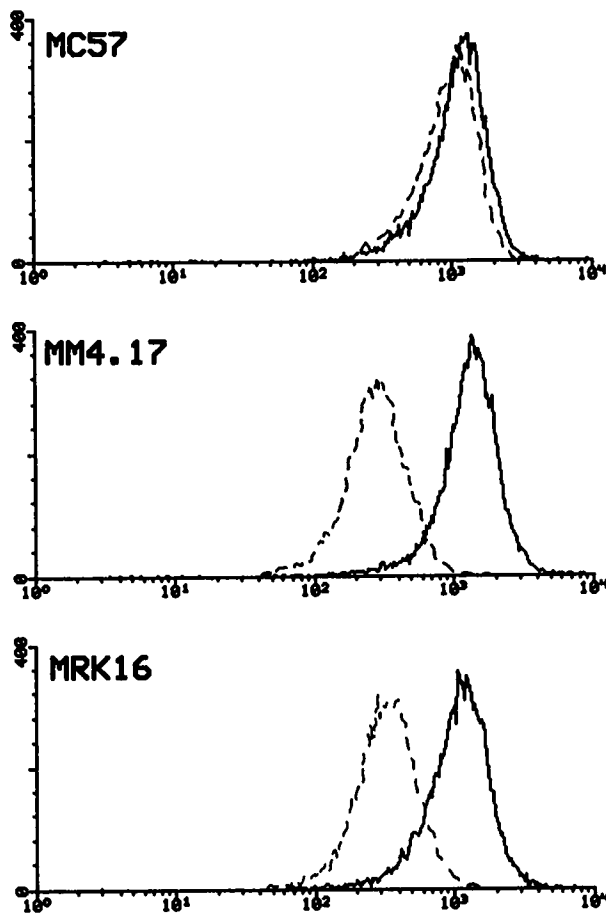


**Figure 2.** Effects of temperature on Pgp detection by three different anti-Pgp mAb. The fluorescence intensities (x-axes, logarithmic scale) are shown as a function of the MDR-cell numbers in each channel (y-axes, linear scale). The MDR-CEM cells were stained with anti-Pgp mAb (MC57, MM4.17 or MRK16) either on ice (dotted lines) or at 37°C (plain lines). The shift of temperature from 0 to 37°C had no effect on the Pgp staining by MC57, whereas it enhanced the intensity of the staining by MM4.17 and MRK16, as well as the homogeneity of the detection mediated by MM4.17.

ture. MRK16 binding was also enhanced by each RMA ( $p < 0.05$ ), but only when the staining was performed on ice. On the contrary, MM4.17-mediated Pgp detection was never affected by RMA, neither at 37 nor at 0°C. The effects of MDR-CEM cells pretreatment with 10  $\mu\text{g}/\text{ml}$  SDZ 280-446 are shown in a representative experiment (Figure 4).

The RMA-pretreatment of the cells could not only enhance the level of the Pgp detection but also its homogeneity (narrower profile for RMA-treated cells versus solvent-treated ones). However, this enhancement was only obtained for MC57 epitope detection, though at both 37 and 0°C (Figures 4 and 5).

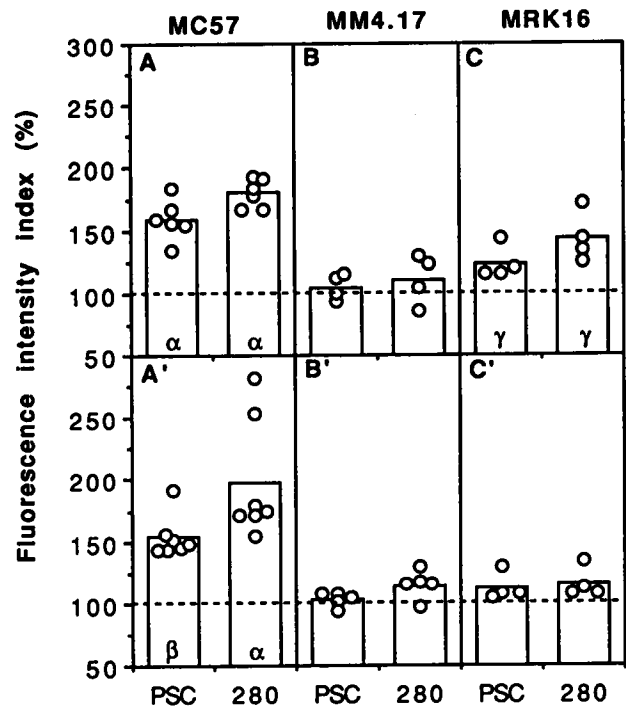


**Figure 3.** Effects of the RMA pretreatment on the intensity of the Pgp detection mediated by three different anti-Pgp mAb. Fluorescence intensities were measured for MDR-CEM cells treated with either SDZ PSC 833 (PSC) or SDZ 280-446 (280) in four to seven individual experiments. They are shown as percentages of the fluorescence intensity of control (solvent-treated) cells, used as 100% standards (dotted line). The PSC and 280 data, obtained in individual experiments, are shown as open symbols whereas the mean values are indicated by the columns. Top panels (A–C) show data obtained with staining performed at 0°C (melting ice) and bottom panels (A'–C') those obtained with staining performed at 37°C. MC57 epitope expression (A and A') was higher on RMA-treated cells, at both temperatures; MM4.17 epitope expression (B and B') was virtually unaffected by the RMA; MRK16 epitope expression (C and C') was increased by SDZ 280-446 and slightly by SDZ PSC 833, but only at 0°C. Significance of the RMA effect on the fluorescence intensity is indicated by greek letters within histograms:  $\alpha$ ,  $p < 0.001$ ;  $\beta$ ,  $p < 0.01$ ; and  $\gamma$ ,  $p < 0.05$  (comparison of the mean fluorescence index values obtained with the RMA treatment to the value of 100, expected in the absence of RMA effect, by using the table of  $t$  distributions).

## Discussion

Pgp-expressing tumor cells actively efflux ACD and develop MDR. Recently, a pulse-treatment of MDR-tumor cells with highly active RMA was shown sufficient to give a long lasting restoration of their DAU retention.<sup>7</sup> Such a strong inhibition of Pgp function might be caused by an RMA-induced Pgp depletion from the MDR-cell plasma membrane, such as mediated by shedding or endocytosis. Using fluores-

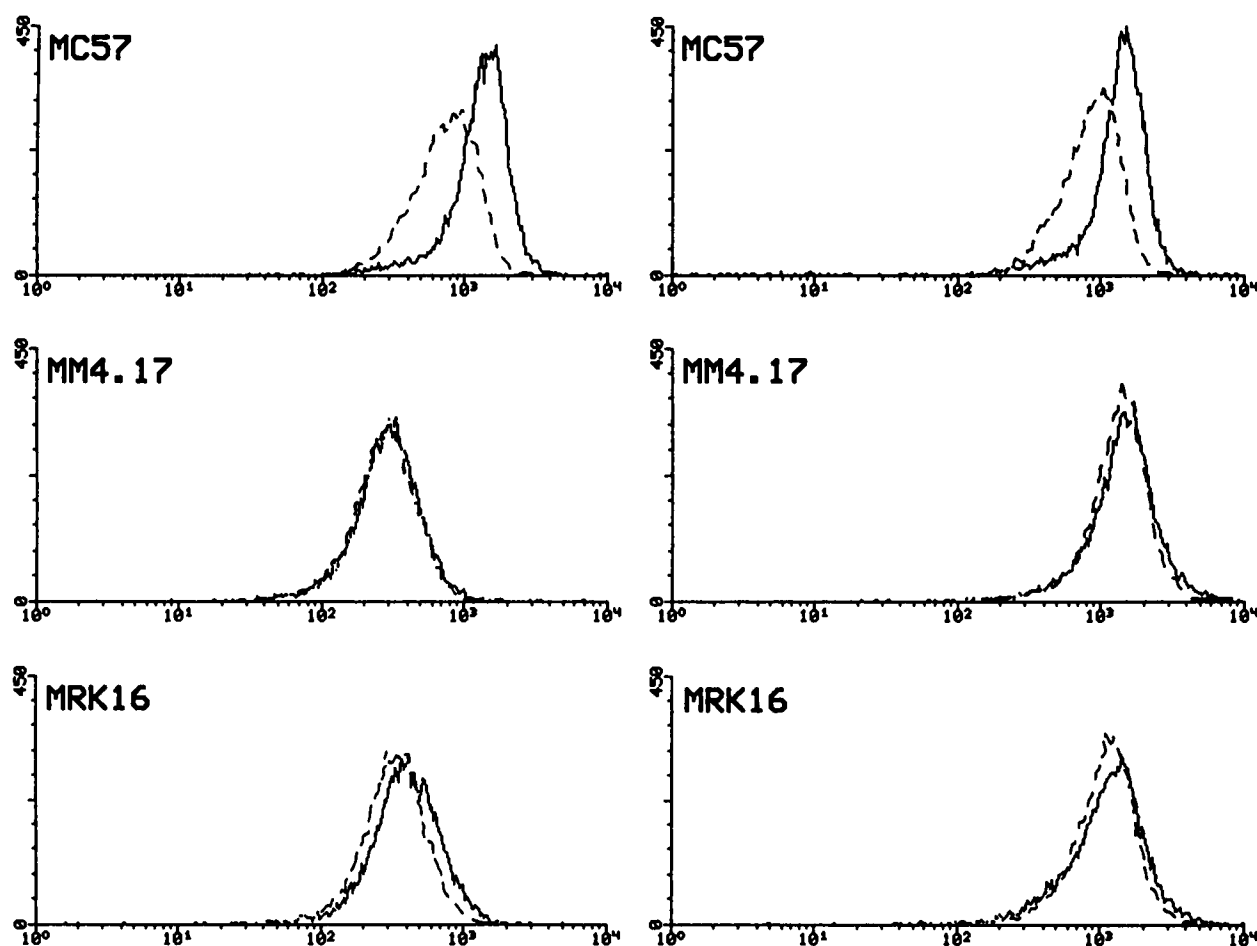


**Figure 4.** Effects of temperature and/or SDZ 280-446 on Pgp detection by three different anti-Pgp mAb. The fluorescence intensities (x- axes, logarithmic scale) are shown as a function of the MDR-cell numbers in each channel (y-axes, linear scale). The MDR-CEM cells were stained with anti-Pgp mAb (MC57, MM4.17 or MRK16) either on ice (left column) or at 37°C (right column); the staining was performed on cells exposed to a short pretreatment with either 10 µg/ml SDZ 280-446 (plain lines) or the control solvent (dotted lines). SDZ 280-446-pretreated MDR-CEM cells expressed higher and more homogenous levels of MC57 epitopes than controls at both temperatures, whereas they expressed slightly higher levels of MRK16 epitopes only when staining was performed at 0°C. On the contrary, no substantial RMA-dependent alterations of the fluorescence profiles of the MDR-CEM cell population were found when detecting the levels of MM4.17 epitopes.

cence microscopy and flow cytometry to study DAU retention and Pgp epitope expression, we now show that the RMA-induced disappearance of Pgp function did not correlate with a lack of Pgp expression on the MDR cell surface: when human MDR-cells (MDR-Lovo, MDR-KB and MDR-CEM) were pretreated with SDZ PSC 833, in conditions where Pgp function was reduced, there was indeed no disappearance of Pgp molecules from the cell surface, as measured by use of anti-Pgp mAb directed against epitopes expressed on the extracellular portions of human Pgp.

On the contrary, SDZ PSC 833 even enhanced the binding of one anti-Pgp mAb to all three tested human MDR-cell lines. That particular anti-Pgp mAb (MC57) was directed against a conformational

epitope expressed on the extracellular portion of Pgp<sup>4</sup> (Cianfriglia *et al.*, in preparation). Further studies with the MDR-CEM cells extended this curious effect to three other RMA (SDZ 280-446, CsA and verapamil). They showed that all tested RMA enhanced MC57 binding and that this effect correlated with their strength for restoring DAU retention or ACD-mediated cell growth inhibition. In this assay, while the weakest RMA, verapamil, had to be present throughout the whole Pgp detection procedure to cause a substantial (35–45%) increase of MC57 binding, a 5 min pretreatment of the MDR-CEM cells with the strongest RMA, SDZ 280-446, was sufficient to give the maximum (about 2-fold) enhancement of MC57 binding. This did not seem to require active metabolism and membrane fluidity during the RMA

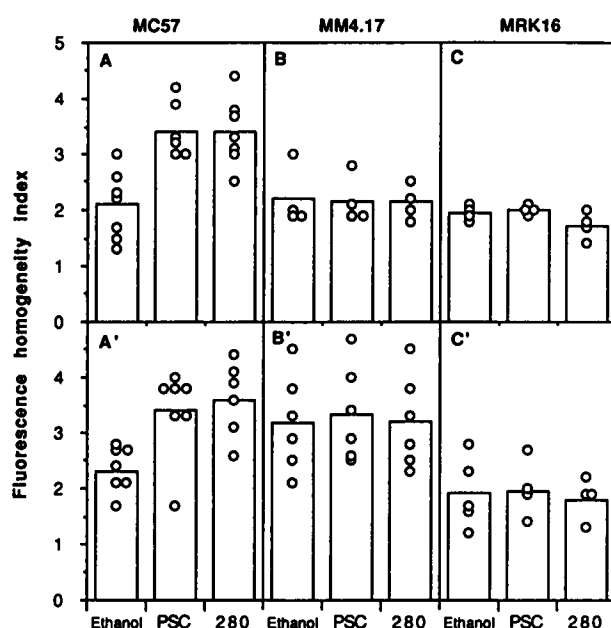


**Figure 5.** Effects of RMA pretreatment and/or staining temperature on the homogeneity (of the cell population profile) of the Pgp detection mediated by three different anti-Pgp mAb. Fluorescence homogeneity indices were measured for MDR-CEM cells treated with either the RMA solvent only (Ethanol), SDZ PSC 833 (PSC) or SDZ 280-446 (280) in four to seven individual experiments. Individual values are shown as open symbols, whereas the mean values are represented by columns. Top panels (A–C) show data obtained with staining performed at 0°C (ice) and bottom panels (A'–C') those obtained with staining performed at 37°C. The homogeneity of the fluorescence profiles of the MDR-CEM cells was increased in two situations: by the RMA, when Pgp detection was performed by MC57 (compare 'PSC' and '280' data with 'Ethanol' data), and by the physiological temperature, when Pgp detection was performed by MM4.17 [compare 'Ethanol' data at 0°C (B) and 37°C (B')]. No effect on MRK16 epitope detection was found.

pretreatment of the cells. The increased mean fluorescence of the RMA-treated cell population was correlated with its higher homogeneity of MC57 binding (narrower fluorescence profile) and its higher DAU retention capacity. However, the amounts of Pgp molecules per cell should actually be similar in untreated and RMA-treated cells. Indeed, RMA-treated cells did not display increased binding of two other anti-Pgp mAb, thus no increased expression of their cognate MM4.17 and MRK16 epitopes. This suggests that RMA only modulated the expression of the MC57 epitope.

Further comparisons showed that not only the RMA, but also the incubation conditions could have different effects on anti-Pgp mAb binding to MDR-cells. While MC57 binding was similar at 0 and 37°C,

the binding of the other two anti-Pgp mAb was higher at 37 than at 0°C. Cells with a normal membrane fluidity (37°C) displayed four times more MM4.17- and MRK16-specific fluorescence than cells with a reduced membrane fluidity (0°C). This might indicate an intrinsically lower availability of the MM4.17 and MRK16 epitopes at a non-physiological temperature. Alternatively, their exposure on the cell surface might be equal at both temperatures but with a topography that would be less favorable for antibody bridging at 0°C, corresponding to a reduced plasma membrane fluidity. Unlike the temperature, RMA pretreatment of the MDR-cells did not enhance the binding of MM4.17, as it did for MC57. MRK16 binding to MDR-cells was slightly enhanced by the RMA pretreatment, but only when the mAb binding was performed on ice (thus, in suboptimal conditions for this epitope) and not when performed at 37°C.

Even in the presence of azide and at 0°C, only a few minutes' exposure of the MDR-CEM cells to the RMA was sufficient to induce a marked enhancement of MC57 binding, suggesting that neither metabolism nor cell membrane fluidity seemed required. Thus, neither new Pgp synthesis nor expression of novel Pgp-containing surface membrane should play a role and the enhanced MC57 epitope expression should have a strictly structural basis. When the RMA addition was done after the MC57 binding step, the enhancing effect of the RMA on the MC57 epitope was lost. This suggested that the RMA enhanced the antigenicity of the MC57 epitope, like the temperature did for the MM4.17 and MRK16 epitopes. Possible interpretations for these curious alterations of Pgp epitope expression will be discussed below, as well as their possible significance for the normal organization of Pgp molecules in the plasma membrane of MDR-cells.

Since all three anti-Pgp mAb were IgG2a of BALB/c origin, the differences observed for MC57, MM4.17 and MRK16 could not be due to FcR interactions but were strictly mediated by the recognition of distinct epitopes on the Pgp molecules. Moreover, no unexpected binding of anti-Pgp mAb was found on the parental cell lines used as controls. Thus, the observed shifts of FACScan-mediated detection of Pgp-expressing cells were actually related to Pgp epitope expression. Therefore, caution must be taken when quantitating Pgp expression by use of anti-Pgp antibodies, as well as when mapping Pgp epitopes. Particularly, membrane active agents such as RMA, and factors which modulate general membrane organization, may differentially influence the detectability of distinct Pgp epitopes.

Like the MRK16 epitope,<sup>6</sup> the MC57 epitope is conformational<sup>4</sup> (Cianfraglia *et al.*, in preparation). Therefore, increased binding of the cognate antibodies might be due to conformational changes in single Pgp molecules or to differences of topographical distribution of Pgp molecules related to their functional status in physiologically intact or altered membranes of MDR-cells.

The increased mean fluorescence of the RMA-treated cell population also correlated with its lower heterogeneity of MC57 binding and its higher DAU retention capacity. The more homogeneous fluorescence profile of the RMA-treated MDR-CEM cell population could be interpreted as follows: the RMA might particularly increase MC57 binding to the fraction of the cells where it was the lowest in the absence of RMA treatment, rather than causing a similar fractional increase of binding on all cells of the population. Productive RMA interactions with the cell membrane pumping machinery (whose Pgp itself might be one element only) could induce changes in the organization of the Pgp molecules. These changes could affect either the access to otherwise cryptic MC57 epitopes, or the structure of the MC57 epitope itself by inducing a higher affinity for its cognate mAb.

However, since MC57 epitopes are conformational, the enhancing effect of the RMA on the MC57 binding might also be interpreted as a RMA-induced change of the organization of Pgp molecules. For example, Pgp molecules might exist in two conformational states, one presenting the MC57 epitope efficiently and the other one less efficiently. The two forms may co-exist and be in equilibrium in the plasma membrane of MDR-cells; the RMA might shift the equilibrium from the second form to the first. In this context, it is interesting that four different RMA (SDZ PSC 833, SDZ 280-446, CsA and verapamil) enhanced MC57 binding on the MDR-CEM cells and that this effect correlated with their strength for restoring DAU retention or ACD-mediated cell growth inhibition. Thus, the Pgp form presenting the MC57 epitope most efficiently would seem to be the inactive (or inactivated) form of the Pgp.

## Conclusion

Lower expression of some Pgp epitopes at a non-physiological temperature (MM4.17 and MRK16) and higher expression of some others in RMA-treated cells (MC57) suggest alterations of the conformation of individual Pgp molecules, their topo-

graphical distribution or polymerization status in the membrane, or modulation of Pgp interactions with other membrane components. Major alterations of membrane structure may account for the temperature-dependent expression of MM4.17 and MRK16 epitopes, but a testable hypothesis may be proposed to integrate the MC57 epitope data. Pgp molecules might have the capacity to form homopolymers and be present in the membrane in two types of structural organization: monomeric and polymeric. Pgp dimers were described<sup>17</sup> and would be functional,<sup>18</sup> the existence of larger oligomers being also suggested.<sup>6</sup> A higher expression of MC57 epitopes on oligomers than on individual Pgp molecules would indicate that RMA caused Pgp aggregation and that optimal pumping function was mediated by individual Pgp molecules with poor MC57 epitope expression. If, on the contrary, a higher expression of MC57 epitopes would occur on single Pgp molecules than on oligomers, our data would indicate that RMA caused disruption of functional Pgp oligomers allowing expression of cryptic MC57 epitopes.

## References

1. Pastan IH, Gottesman MM. Molecular biology of multidrug resistance in human cells. *Import Adv Oncol* 1988; **1**: 3-16.
2. Georges E, Sharom FJ, Ling V. Multidrug resistance and chemosensitization: therapeutic implications for cancer chemotherapy. *Adv Pharmacol* 1990; **21**: 185-220.
3. Higgins CF, Gottesman MM. Is the multidrug transporter a flippase? *Trends Biochem Sci* 1992; **17**: 18-21.
4. Cenciarelli C, Currier SJ, Willingham MC, *et al.* Characterization by somatic cell genetics of a monoclonal antibody to the MDR1 gene product (P-glycoprotein): determination of P-glycoprotein expression in multidrug-resistant KB and CEM cell variants. *Int J Cancer* 1991; **47**: 533-43.
5. Cianfriglia M, Willingham MC, Tombesi M, *et al.* P-glycoprotein epitope mapping. 1. Identification of a linear human-specific epitope in the fourth loop of the P-glycoprotein extracellular domain by MM4.17 murine monoclonal antibody to multidrug resistant cells. *Int J Cancer* 1993; **56**: 153-60.
6. Georges E, Tsuruo T, Ling V. Topology of P-glycoprotein as determined by epitope mapping of MRK-16 monoclonal antibody. *J Biol Chem* 1993; **268**: 1792-8.
7. Boesch D, Loor F. Extent and persistence of P-glycoprotein inhibition in multidrug-resistant P388 cells after exposure to resistance-modifying agents. *Anti-Cancer Drugs* 1994; **5**: 229-38.
8. Gavériaux C, Boesch D, Jachez B, *et al.* SDZ PSC 833, a non-immunosuppressive cyclosporin analog, is a very potent multidrug-resistance modifier. *J Cell Pharmacol* 1991; **2**: 225-34.

9. Jachez B, Nordmann R, Loor F. Restoration of taxol-sensitivity of multidrug-resistant cells by the cyclosporine SDZ PSC 833 and the cyclopeptolide SDZ 280-446. *J Natl Cancer Inst* 1993; **85**: 478-83.
10. Loor F, Boesch D, Gavériaux C, *et al.* SDZ 280-446, a novel semi-synthetic cyclopeptolide: *in vitro* and *in vivo* circumvention of the P-glycoprotein-mediated tumour cell multidrug resistance. *Br J Cancer* 1992; **65**: 11-8.
11. Shen DW, Cardarelli C, Hwang J, *et al.* Multiple drug-resistant human KB carcinoma cells independently selected for high level resistance to colchicine, adriamycin, or vinblastine show changes in expression of specific proteins. *J Biol Chem* 1986; **261**: 7762-70.
12. Grandi M, Geroni C, Giuliani FC. Isolation and characterization of a human colon adenocarcinoma cell line resistant to doxorubicin. *Br J Cancer* 1986; **54**: 515-8.
13. Gekeler V, Frese G, Diddend H, *et al.* Expression of a P-glycoprotein gene is inducible in a multidrug-resistant human leukemia cell line. *Biochem Biophys Res Commun* 1988; **155**: 754-60.
14. Gekeler V, Weger S, Probst H. MDR1/P-glycoprotein gene segments analyzed from various human leukemic cell lines exhibiting different multidrug resistance profiles. *Biochem Biophys Res Commun* 1990; **169**: 796-802.
15. Jachez B, Loor F. Atypical multi-drug resistance (MDR): low sensitivity of a P-glycoprotein-expressing human T lymphoblastoid MDR cell line to classical P-glycoprotein-directed resistance-modulating agents. *Anti-Cancer Drugs* 1993; **4**: 605-15.
16. Boesch D, Muller K, Pourtier-Manzanedo A, *et al.* Restoration of daunomycin retention in multidrug-resistant P388 cells by submicromolar concentrations of SDZ PSC 833, a nonimmunosuppressive cyclosporin derivative. *Exp Cell Res* 1991; **196**: 26-32.
17. Boscoboinik D, Debanne MT, Stafford AR, *et al.* Dimerization of the P-glycoprotein in membranes. *Biochim Biophys Acta* 1990; **1027**: 225-8.
18. Naito M, Tsuruo T. Functionally active homodimer of P-glycoprotein in multidrug-resistant tumor cells. *Biochem Biophys Res Commun* 1992; **185**: 284-90.

(Received 19 July 1994; received in revised form 21 September 1994; accepted 23 September 1994)